# Critical Exponents in Cytosolic Diffusion

Robert Marsland
(Dated: May 16, 2014)

The interior of a cell is very crowded (up to 35% protein by weight), with significant consequences for diffusive transport. The possible trajectories of a given tracer particle are constrained by the labyrinth of obstacles. For a static obstacle configuration, a percolation transition takes place at a certain critical obstacle density, so that above this density no long-range transport is possible. A scaling relation links the critical exponent $\mu$ for the vanishing of the diffusion coefficient at this transition to the exponent $\nu$ for divergence of the correlation length and the exponent $\alpha$ characterizing subdiffusive transport on scales $\ll \xi$. Here I derive this relation, and compare it to data from simulation and experiment.

In order to grow, replicate, and adapt to its environment, a cell has to move molecules to specific places at the right times. In eukaryotic cells, some of this motion is due to active transport, using molecular motors - whether on a microtuble track or through a "stirring" effect resulting from contractions of a network of smaller filaments throughout the cytosol. But thermal diffusion is still the primary mechanism for moving many molecules around the cell, especially in bacteria, which lack the tools for active transport except in the specific context of preparation for cell division (cf. [3]). Diffusion in the cell is very different from diffusion in vitro, because the cell is a very crowded place. The concentration of proteins is so high that the cytosol more closely resembles a protein crystal than it does a dilute in vitro solution [2]. This crowding constrains the possible paths of a given tracer molecule, radically altering the bulk transport properties of the medium.

If these obstacles that generate these constraints are pinned to fixed positions, there will be a critical density of obstacles above which no long-range transport is possible, because none of the allowed paths from any starting point extend across the whole cell. Just below this density, correlations in the particle trajectories induced by the constraints will cause deviations at short times from the ordinary linear scaling of the mean-squared displacement with time. The behavior of the diffusion coefficient near this critical point will be linked to the the short-time subdiffusive transport exponent by a scaling relation, as discussed in [4].

In the first section of this paper I derive this scaling relation and explain what it means. In the second section, I numerically simulate an in vivo diffusion experiment to test this prediction. In the third section I will compare the theory to actual data from the literature.

## I. SCALING THEORY

We can start by recalling the fundamental reason why at sufficiently small length scales the motion of a tracer particle in a crowded environment should be subdiffusive. The constraints on allowed paths imply that the mean and variance in the displacement $\Delta\mathbf{r}(t_i)$ of the particle during a given small time increment $[t_i, t_i + \Delta t]$ depend on where it is in the "labyrinth" of possible trajectories. If it is at a dead-end, for example, the mean displacement will have to be in the direction away from the dead end, and the variance will be smaller than at a node where all directions of motion are possible. But the location of the particle within the labyrinth depends on its history, and so there will be correlations among the displacement vectors at different times. These correlations modify the scaling of the mean-squared displacement (MSD) $\langle \Delta R^2 \rangle$ with time:

$$\begin{aligned}\langle \Delta R^2(t) \rangle &= \sum_{i,j=1}^{N} \langle \Delta\mathbf{r}(t_i) \cdot \Delta\mathbf{r}(t_j) \rangle \\ &= N \left( \langle \Delta\mathbf{r}^2 \rangle + \sum_{i=2}^{N} \langle \Delta\mathbf{r}(t_1) \cdot \Delta\mathbf{r}(t_i) \rangle \right) \\ &\propto N^\alpha \propto t^\alpha \text{ for } a^2 \ll \langle \Delta R^2 \rangle \ll \xi^2\end{aligned}$$

The dead ends and labyrinthine turns make the correlations in the second term on the second live nonzero and negative, since they decrease the probability of continuing on in the same direction for many time steps in a row. These correlations will die off as the time interval increases, but if $N$ is sufficiently small that $\langle \Delta\mathbf{r}(t_1) \cdot \Delta\mathbf{r}(t_N) \rangle$ is still non-negligible compared to $\langle \Delta\mathbf{r}^2 \rangle$, then the value of the sum will be a function of $N$. On length scales much larger than the typical obstacle size $a$ but much smaller than the characteristic length $\xi$ over which the correlations decay, we expect the path of the particle to be scale-free, so that the displacement grows as some power $\alpha$ of the number of steps (which is proportional to the time $t$ from when the particle started diffusing).

If on the other hand we look at length scales $\gg \xi$, we expect the system to look homogeneous, and for normal diffusion to be recovered. We can understand this mathematically by noting that when $N$ is large enough that $\langle \Delta\mathbf{r}(t_1) \cdot \Delta\mathbf{r}(t_N) \rangle \ll \langle \Delta\mathbf{r}^2 \rangle$, then as long as the correlations are dying off exponentially the upper limit of the sum index can be taken to infinity without significantly changing the value of the sum. This means that the sum in the second term is independent of $N$, so the whole expression in parentheses is a constant, and $\langle \Delta R^2(t) \rangle \propto N \propto t$.

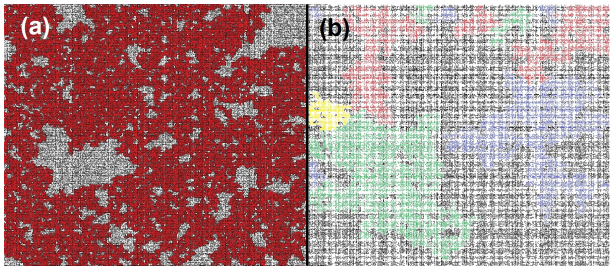


FIG. 1. Typical obstacle configurations on a square lattice near the critical point. From a given site, each of the four nearest neighbors is accessible with probability $p$, and is blocked with probability $1-p$. **(a)** $p = 0.51$. Untrapped region ('infinite cluster') shaded red. **(b)** $p = 0.49$ (generated from panel (a) by taking advantage of duality, and shading bonds instead of voids). There is no untrapped region, but some of the largest traps are shaded in different colors.

The scale $\xi$ characterizing the exponential decay of these correlations as a function of distance is the same as the typical size of the "traps" in the medium: regions that are completely surrounded by obstacles, and cannot be entered or exited without obstacle rearrangement (see figure 1). Once you have moved to the border of the next trap, the probability of hitting a dead end or sharp bend no longer depends on the route you took around the previous trap. $\xi$ increases as the system becomes more crowded. Eventually, $\xi$ becomes comparable to the volume of the cell, so that the diffuser is always moving around the same trapped area, and never reaches normal diffusion.

When $\xi$ is still smaller than the cell size, the mean time it takes to travel this distance and cross over from subdiffusive to diffusive behavior is the cross-over time $t_x$. For $\xi \gg a$, the bulk of the time spent crossing $\xi$ will be in the power law regime with $\langle \Delta R^2 \rangle \propto t^\alpha$, so $t_x \sim \xi^{2/\alpha}$. We can model the coarse-grained diffusion as a random walk that takes steps $\xi$ in uncorrelated directions in a time $t_x$, so that $D = \xi^2/t_x$.

To model the MSD we expect to observe in a typical experiment, however, we need to account for the possibility that our tracer particle might have started in a trapped region. Instead of sorting through all the data to try to identify and throw out the trials where the particle is trapped, we can just include them in the average, and multiply our original MSD prediction by the probability $P_\infty$ that the tracer particle is not in a trap.

Thus we find:

$$D = P_\infty \frac{\xi^2}{t_x} = P_\infty \xi^{2-2/\alpha} \tag{1}$$

If we characterize the degree of crowding by some continuous parameter $\phi$, then for a static configuration of obstacles, there will be a critical value $\phi_c$ above which diffusion becomes impossible, and all the particles are trapped (see figure 1). Near $\phi_c$, $D$, $P_\infty$, and $\xi$ will be proportional to some power of $\epsilon = \phi_c - \phi$, with $D$ vanishing with power $\mu$, $P_\infty$ vanishing with power $\beta$, and $\xi$ diverging with power $-\nu$:

$$D \propto \epsilon^\mu$$
$$P_\infty \propto \epsilon^\beta$$
$$\xi \propto \epsilon^{-\nu}.$$

These exponents are unchanged if we replace $\phi$ by some other parameter that is an analytic function of $\phi$ at $\phi_c$. So $\phi$ could be the volume fraction of obstacles (its usual definition), or the salt concentration in the environment, or even the pressure exerted on a cell being squeezed between two plates.

Using (1), we can thus conclude that near $\phi_c$,

$$D \propto \epsilon^{-\nu(2-2/\alpha)+\beta}$$

or

$$\mu = -\nu(2 - 2/\alpha) + \beta. \tag{2}$$

This is equivalent to equation (19) of [4], with the notational replacement $\alpha = 2/d_w$. $\nu$ and $\beta$, given on the left hand side of table I, are universal exponents, that only depend on the dimensionality of the system. $\alpha$ and $\mu$ also takes universal values on lattices, but they can deviate from these in continuum models, like the popular "swiss cheese" model of random overlapping spherical obstacles [4]. Equation (2) tells us that if we observe our system on a small enough length scale to see the sub-diffusion and measure the exponent $\alpha$ (which requires that we are close enough to the critical point to have $\xi \gg a$), we should be able to predict the exponent $\mu$ with which $D$ drops to 0 as $\phi \to \phi_c$.

| | $\nu$ | $\beta$ | $\alpha$ | $\mu$ |
|---|---|---|---|---|
| d=2 | 4/3 | 5/36 | 0.70 | 1.3 |
| d=3 | 0.88 | 0.41 | 0.53 | 2.0 |

TABLE I. Critical percolation exponents: $\nu$ and $\beta$ are universal, and $\alpha$ and $\mu$ are the universal values on lattices. $\nu$, $\beta$ and $\mu$ as reported in [6]. $\alpha$ computed using 2, equivalent to equation (19) in [4].

## II. MODEL AND SIMULATION

We can see the physical significance of these results through a simulation of diffusion on a square or cubic lattice with some fraction of bonds between lattice sites randomly blocked to represent the obstacles. By universality, this should produce the same values of $\nu$ and $\beta$ as would be measured in a more realistic continuum system of static obstacles, so $\alpha$ and $\mu$ should obey the same quantitative relationship with each other.

The simulation starts by randomly connecting nearest neighbors in the lattice with probability $p$ for each bond.

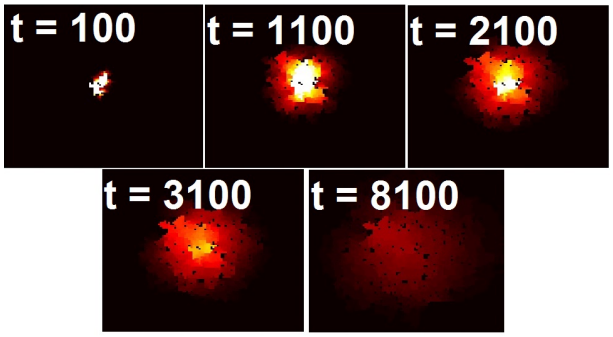


FIG. 2. Frames from movie of simulation data of 2 dimensional diffusion with $p = 0.6$. Each unit of time is a single iteration of equation (3). Concentration as a function of position is represented by light intensity, as in an experiment with fluorescently tagged proteins.

A connectivity matrix $b_{ij}$ records which lattice sites are connected, with $b_{ij} = 1$ if $i$ and $j$ are connected and 0 if they are not. A concentration profile is initialized by assigning a concentration $c_i$ to each lattice point. At each time step, the concentration spreads uniformly through all the open bonds, via the equation

$$c_i(t_{n+1}) = c_i(t_n) + \frac{1}{z}\sum_{\langle j\rangle} b_{ij}[-c_i(t_n) + c_j(t_n)] \qquad (3)$$

where the sum is over all the $j$'s that are nearest neighbors to $i$, and $z$ is the total number of nearest neighbors (4 for the square lattice, 6 for the cubic).

We can use this framework to simulate a simple in vivo diffusion experiment, where a protein of interest is fused to a photo-switchable green fluorescent tag. A pulse of laser light at the appropriate frequency in a small region of the cell (at position $\mathbf{r} = 0$) converts the green fluorescence to red, and the newly red proteins spread throughout the green background. The "bond probability" $p$ now corresponds to the probability that there is an open passage between two neighboring voids in the sea of obstacles, and is an analytic function of the obstacle density. The obstacle density could be controlled in the experiment by varying salt concentrations in the environment of the cell, or by physically squishing a cell with a sufficiently resilient cell wall. Figure 2 shows a few frames from the movie that would be generated by such an experiment.

Figure 3 shows the MSD vs. time on a log-log plot for eight different values of the bond probability $p$, in two dimensions. The localization transition is very clear - we can see that below $p_c = 1/2$ the MSD levels off at a finite value at long times (equal to the correlation length $\xi$), while above $p_c$, all the traces eventually reach a slope of 1. Right at $p_c$, the slope appears to asymptote to something near $\alpha = 0.7$, although the simulation was not run long enough to confirm convergence to that value.

We can find the diffusion coefficient $D$ in units of [lattice spacing]$^2$/[time step] by dividing the MSD by $4t$ at a

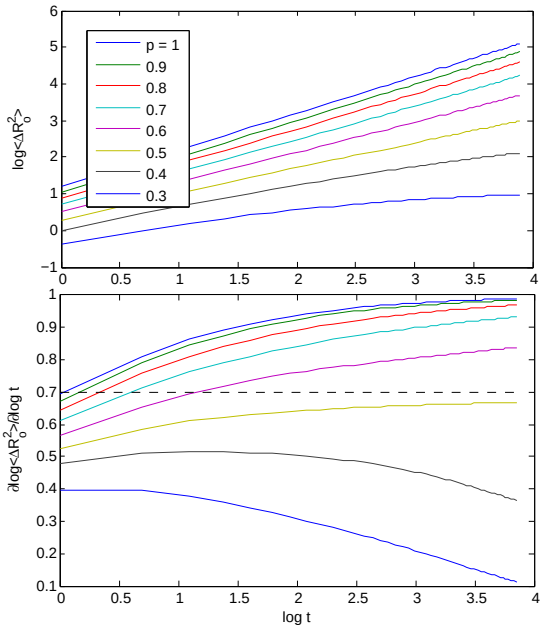


FIG. 3. (a) MSD vs. time for different values of the bond connection probability $p$. (b) Derivatives of these traces. The behavior of the derivative at $p_c = 0.5$ is consistent with an asymptotic approach to $\alpha = 0.7$.

time $t$ large enough that the log-log plot is well in the diffusive regime with slope 1. I plotted $\log D$ vs. $\log(p - p_c)$ for 8 values of $p$ between .65 and 1. At each value of $p$, 100 trials were simulated for 2500 time steps, and the slopes were plotted to ensure that the time was long enough to reach the diffusive regime. $\log D$ decreased from 2.1 to 0.84 over these 8 points, with a slope of $\mu = 1.1$ in a good linear fit (the RMS of the residuals was 0.02). This is significantly different from the value of 1.30 reported in the literature and predicted by the scaling relation. This is probably due to the fact that $\xi \sim a$ for the $p$ values that I used, and so $t_x$ is not dominated by scale-free transport with exponent $\alpha$. It takes a long time to obtain good values for $D$ at $p$ close to $p_c$, because the crossover time $t_x$ to normal diffusion diverges.

## III. COMPARISON WITH DATA

An experiment similar in spirit to the one described above has been carried out on GFP in E. Coli [5]. The diffusion coefficient was measured after exposing the bacteria to media with varying NaCl concentrations, with results as plotted in 4. When the cell is exposed to a higher salt concentration than the one in which it was grown, the cytoplasm shrinks and the density of obstacles to diffusion increases. At a critical concentration somewhere less than 0.5 M, diffusion stops and the GFP are permanently localized (on the time scale of the exper-

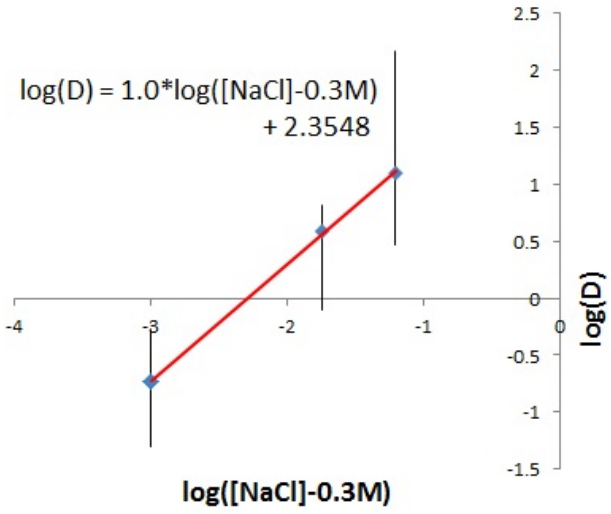


FIG. 4. Data from table S1 in [5]. [NaCl] axis is offset before taking log so that 0 corresponds to the critical concentration. Error bars indicate the interquartile region, or the region where the middle half of the measurements fall. The critical concentration $[\mathrm{NaCl}]_c$ was not measured, but it is less than 0.5 M, because the GFP was observed to be completely immobilized (up to experimental precision) at that concentration. The choice of $[\mathrm{NaCl}]_c$=0.3 M gave the best linear fit, and an exponent of $\mu = 1$. Other choices yield different values, ranging between 1 and 2.5.

iment, which gave an upper bound of $D = 0.001\mu m^2/s$). A linear fit to the plot of $\log D$ vs. $\log([\mathrm{NaCl}]_c\text{-}[\mathrm{NaCl}])$ should yield the critical exponent $\mu$, as long as the measurements were done close enough to the critical point to avoid the problems I had with the simulation. The data from the actual experiment is insufficient for obtaining meaningful constraints on the possible values of $\mu$, however, both because of the small number of concentrations sampled and the large uncertainty at each concentration.

The measurement was performed inversely to the experiment described in the previous section: the authors photobleached the GFP in a small region of the cell, and watched the unbleached GFP diffuse *into* that region. In principle, one could measure the MSD as a function of time with this method, by simply inverting the picture and plotting the spreading of "negative fluorescence intensity" from the bleached site. If one could average over a large enough number of cells and bleach a small enough region for non-uniformities in the inital condition to be negligible, it would be possible to extract $\alpha$ and compare with the scaling relation.

## IV. CONCLUSION

We have described how the results of percolation theory can be applied to extract some general characteristics of particle transport in a model of the cytosol as a bag of fixed rigid obstacles. The primary defect of this model is the assumption of immobility. Many objects of interest in the bacterium's cytosol are about the same size as the main obstacles, and move at the same speeds. This means there is no longer be any permanent confinement at obstacle densities below the random close-packing density, because eventually the obstacles willl rearrange themselves in such a way that the tracer particle can escape.

The consequences of obstacle mobility have been explored in numerical studies. For obstacles undergoing Brownian motion, these studies confirm that normal diffusion is restored on long enough time scales at all obstacle densities [1]. Experimental studies have also been performed on tagged particles diffusing in dense colloids near the "jamming" transition (cf. [7]), where the volume fraction of colloidal particles becomes so high that an individual particle cannot move without rearranging its neighbors. As expected, the log-log plot of MSD vs. time initially levels off at the typical trap size (which is on the order of the particle size in the cited experiment), and then increases again with a slope approaching 1 for time scales long enough for the obstacles to lose memory of the initial configuration. It would be interesting to generalize this scaling theory to this case by introducing the correlation time for the obstacle configuration as an additional time scale.

[1] H. Berry and H. Chaté. Anomolous diffusion due to hindering by mobile obstacles undergoing Brownian motion or Orstein-Ulhenbeck processes. *Phys. Rev. E*, 89:022708, 2014.
[2] A.B. Fulton. How crowded is the cytoplasm? *Biophys. J.*, 30:345–347, 1982.
[3] I. Golding and E.C. Cox. Physical nature of bacterial cytoplasm. *Phys. Rev. Lett.*, 96:098102, 2006.
[4] F. Höfling, T. Munk, E. Frey, and T. Franosch. Critical dynamics of ballistic and Brownian particles in a heterogeneous environment. *J. Chem. Phys.*, 128:164517, 2008.
[5] J.T. Mika, G. van den Bogaart, L. Veenhoff, V. Krasnikov, and B. Poolman. Molecular sieving properties of the cytoplasm of Escherichia coli and consequences of osmotic stress. *Molecular Microbiology*, 77:200, 2010.
[6] D. Stauffer and A. Aharony. *Introduction to Percolation Theory*. Taylor & Francis, Washington, DC, 1992.
[7] E.R. Weeks and D.A. Weitz. Subdiffusion and the cage effect studied near the colloidal glass transition. *Chem. Phys.*, 284:361, 2002.